X-ray absorption fine structure studies of buried Ge–Si interfaces

P. Aebi, T. Tyliszczak, and A. P. Hitchcock

Institute for Materials Research and Ontario Centre for Materials Research, McMaster University, Hamilton, Canada

T. E. Jackman and J-M. Baribeau

Institute for Microstructural Sciences, National Research Council, Ottawa, Canada

We have used Ge K-edge x-ray absorption fine structure (EXAFS) and a gas ionization detector with sample rotation to study the local environment of nominally pure Ge layers buried in single crystal Si. The samples were grown by molecular-beam epitaxy on Si(100). The dependence on thickness, number of Ge layers and growth temperature is explored. Considerable sensitivity to the quality of the epitaxial growth is observed. For instance the degree of mixing of the Si and Ge layers is a function of the growth temperature. A weak polarization dependence of the Ge K-edge EXAFS is observed. The initial quantitative analysis provides estimates of intermixing in the thinnest layers which are compatible with results of complementary Raman measurements.

I. INTRODUCTION

Si–Si$_{1-x}$Ge$_x$ strained layer superlattice structures have been used successfully in a number of new devices such as heterojunction bipolar transistors. Interest has grown recently in very short period (Si$_m$Ge$_n$)$_p$ atomic layer superlattices (ALS) made of p periods of alternating m and n monolayers of *pure* Si and Ge. These materials have the potential to exhibit optical properties not observed in the bulk or alloy materials due to zone folding effects. Characterization of the geometric and electronic structure of ALS samples is very difficult but essential in order to optimize the growth procedures.

Raman scattering has been utilized to investigate ALS samples.[1] Acoustic phonons have been found to be sensitive to the overall periodicity and average properties while optical phonons yield information regarding local structure, interface smearing, and lattice-strain effects. Unfortunately these parameters are coupled in the analysis and caution is required in the interpretation of the Raman data.[2] Independent measurements of certain parameters, such as the number of Ge–Ge, Si–Ge, or Si–Si bonds, their bond lengths, and the local strain environment would be extremely useful in analyses of the Raman data. To this end we have initiated a study to determine if x-ray absorption fine structure (EXAFS) at the Ge K-edge (11,104 eV) can supply some of the information discussed above. In principle, bond lengths accurate to 0.02 Å, coordination numbers to 20% and elemental identity to within 2 Z-units can be obtained using EXAFS.[3,4]

We have measured the EXAFS signal for a series of (Si$_m$Ge$_n$)$_p$ samples grown by molecular-beam epitaxy (MBE) under different growth conditions. The Raman scattering, double crystal x-ray diffraction and glancing incidence x-ray diffraction of these samples have been measured previously.[5-7] The EXAFS results are found to be sensitive to interdiffusion at the Ge/Si interface. In addition we have investigated the extent to which polarization dependent measurements—i.e., recording Ge EXAFS for sample orientations with the polarization perpendicular or parallel to the

Ge layers—can give additional information. In this brief paper, we report the qualitative interpretation of the data and a preliminary quantitative comparison of the EXAFS data for one sample with the Raman results for the same sample.

II. EXPERIMENTAL

A. Sample preparation

The epitaxial layers were grown in a VG Semicon V80 MBE system on 100 mm Czochralski (100) Si wafers.[5] To ensure identical initial conditions, a thick Si buffer layer was grown at $\approx$520 °C using optimum growth conditions. The substrate temperature was then reduced before the thin Si and Ge epitaxial layers were deposited at rates between 0.02 and 0.04 nm/s. For the samples studied, the growth temperature for the single layers was $\approx$385 °C while for the superlattices the temperature was significantly lower (250–300 °C). Cross comparisons using Rutherford backscattering, secondary ion mass spectrometry, cross-sectional transmission electron microscopy, and x-ray diffraction measurements have established the Ge concentration and nominal layer thicknesses (i.e., ignoring any intermixing).[5,6]

B. Electron yield

The experiments were performed at the A3 and C2 beam lines at the High Energy Synchrotron Source at Cornell University (CHESS). Electron yield detection[8] allows study of the local environment of atoms near the surface ($<0.1\,\mu$m) because of the limited escape depth of the Auger and secondary electrons produced in the decay of the core hole. A special gas-flow electron detector with sample rotation[8-10] is used in order to eliminate diffraction artifacts while providing gas-amplification of the electron yield signal.

Horizontally polarized x rays coming from the double crystal monochromator first traverse a N$_2$ ionization chamber and then enter the gas-flow chamber which contains the sample rotating at 100 rpm. He gas at atmospheric pressure is used because it has a low ionization cross section for x rays and an adequate electron impact ionization cross

section for detection of the high energy Auger and thermalized secondary electrons which escape from the sample. In order to investigate polarization and angle of incidence dependence of the electron yield signal, the gas-flow chamber, with its incorporated rotating sample holder, is mounted on a stepping motor controlled, two circle goniometer.

C. The EXAFS technique

EXAFS is the energy dependent interference of the outgoing photoelectron wave created by x-ray absorption above inner-shell (core) ionization thresholds (edges) with that component backscattered from nearby atoms. In a one particle, single scattering picture[3] the EXAFS signal for polarized x rays may be represented as

$$\chi(k) = \sum_i 3 \cos^2 \Theta_i \cdot \chi_i(k)$$

$$= \sum_i 3 \cos^2 \Theta_i \cdot A_i(k)(N_i/k \cdot r_i^2)$$

$$\times \exp(-2k^2 \sigma_i^2) \sin[2kr_i + \delta_i(k)],$$

where the direction of the ith neighbor with EXAFS component $\chi_i(k)$ makes an angle of Θ_i with the x-ray polarization vector. $A_i(k)$ is the backscattering amplitude as a function of wave number $(k \ (\text{Å}^{-1}) = [0.263(E - E_0)]^{1/2}$, where E_0 is the photon energy (in eV) at which the photoelectron has zero kinetic energy) from each of the neighboring atoms of type i, which are located at a distance r_i and which have a mean-square relative displacement of σ^2. This expression assumes Gaussian distributions of interatomic distances and ignores inelastic and multiple scattering intensity losses. The EXAFS signal depends not only on the energy (wave number) of the photoelectron but also on the distance and number of backscatterers in each shell. The type of backscatterer (i.e., atomic number, electronic structure) determines the backscattering amplitude and phase. The experimental amplitude is attenuated by thermal motion and static disorder (σ, a Debye–Waller-like term, which is the mean relative displacement along the absorber-backscatterer direction) and by inelastic scattering (λ, the mean free path). The EXAFS signal corresponding to individual coordination shells can be isolated using Fourier filtering. Quantitative structural parameters relating to this signal can then be derived using curve fitting based on backscattering amplitudes and phases for the Ge–Ge and Ge–Si components derived either from analysis of the experimental spectra of model compounds or from spherical wave calculations.[11,12]

Figure 1 shows the amplitude functions for Si and Ge backscattering as predicted by spherical wave calculations.[11] The deep minimum at 4 Å^{-1} in the Ge backscattering corresponds to the maximum in the Si backscattering. Thus the EXAFS signal at 4 Å^{-1} turns out to be a very useful semiquantitative indicator for the relative amount of Si in the first shell. This has guided our initial qualitative interpretation of the spectra.

The Ge K-edge EXAFS is the average over the local environment of the Ge atoms in all layers. For the ideal case of a bilayer of pure Ge, the Ge atoms will have an equal number of Ge and Si nearest neighbors. For thicker epilayers there
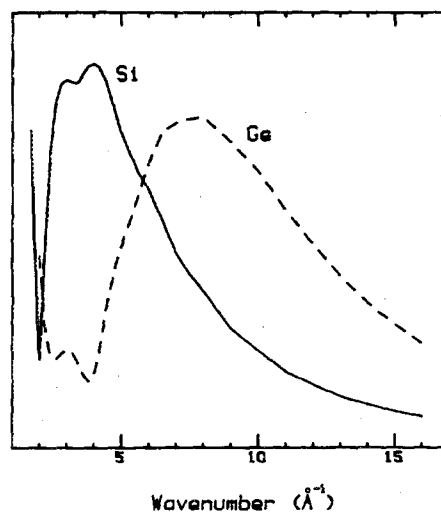

FIG. 1. Backscattering amplitudes for Ge and for Si according to spherical wave calculations.[11]

will be Ge atoms in the interior which will have only Ge nearest neighbors. As discussed above, the shape of the backscattering amplitude can be used to differentiate between Ge and Si backscatterers and thus to establish the ratio of Si:Ge nearest neighbors. Effects such as interdiffusion at an interface will alter this expected ratio and will be evident in the measured spectrum. In addition, from a determination of the bond lengths for different layer thicknesses, information can be obtained about strain/relaxation processes. Alternatively, if the local structure is spatially anisotropic (as might be expected for strained Ge thin films embedded in Si) the polarization dependence of the backscattering intensities can give additional information.[4]

III. RESULTS AND DISCUSSION

A. Qualitative analysis

Figure 2 presents the k^1-weighted, background subtracted k-space EXAFS spectra for the single epilayer and ALS samples for a range of Ge$_n$ thicknesses. The spectra for a 14 at. % Ge–Si alloy and for single crystal Ge are also shown to supply reference spectra of a mostly Si like and a fully Ge environment, respectively. All of these spectra were recorded with the E vector in the plane of the Ge layers. The k-space spectra of the single layers, each of which is the sum of several scans, were Fourier filtered between 0 and 6 Å^{-1} to remove some high frequency noise. The spectra of the multilayer ALS samples, which are of very high quality, were recorded in a single 10 min scan. Figure 3 presents the magnitudes of the Fourier transforms (FT) of the spectra shown in Fig. 2. These are pseudoradial distribution functions— i.e., the radially averaged atom density surrounding the core ionized atom with the peak positions shifted to lower R because of scattering phase shifts.[3]
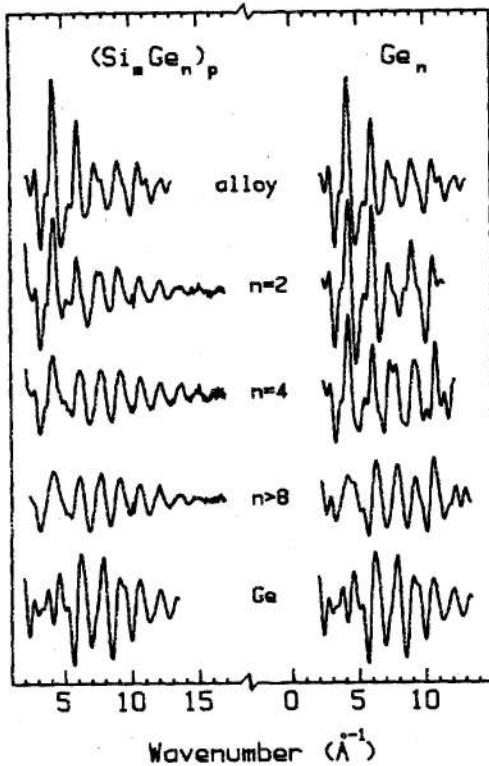
FIG. 2. $k^1\chi(k)$ Ge K-edge EXAFS for MBE-grown $(Si_m Ge_n)_p$ atomic layer superlattice (ALS) structures and Ge_n single layers buried in Si. The values of (m,n,p) for the $n=2$, $n=4$ and $n=8$ ALS samples are: (6,2,48), (9,4,24), and (18,8,8). The $n>8 Ge_n$ layer is an $n=12$ sample. For comparison, the results for a 14 at. % Ge–Si alloy and single crystal Ge are also shown. The k-space data for the single layer Ge_n samples have been Fourier filtered over 0 to 6 Å to remove some high frequency noise.

FIG. 3. Magnitudes of the Fourier transforms of the Ge K-edge EXAFS for the $(Si_m Ge_n)_p$ and Ge_n superlattice structures buried in Si whose EXAFS data is presented in Fig. 2 (see caption to Fig. 2 for sample details).

Although multi- and single epilayer samples of the same layer thickness (n value) which are of equivalent quality (dislocation density, degree of intermixing) would be expected to have an identical Ge local environment and thus identical Ge K-edge EXAFS, our results for the multi- and single layer samples of the same epilayer thickness are quite different. The single layer spectra always exhibit a larger Si backscattering contribution. We interpret this to indicate a much larger extent of intermixing in the single layer than in the multilayer samples. This is more likely a reflection of the higher growth temperatures employed for the single layers than for the ALS, rather than any fundamental dependence on the degree of repetition of the layer structure.

For the ALS multilayer structures, a transition takes place between $n=2$ and $n=8$ from a mixed (Si,Ge) towards a Ge-dominated first shell. This is particularly visible in the FT (Fig. 3) where the centroid of the first shell peak shifts to higher R for $n=4$ and $n=8$. As n increases the contribution from the Si neighbors at the interface decreases but for $n=8$, the 12.5% contribution to the first
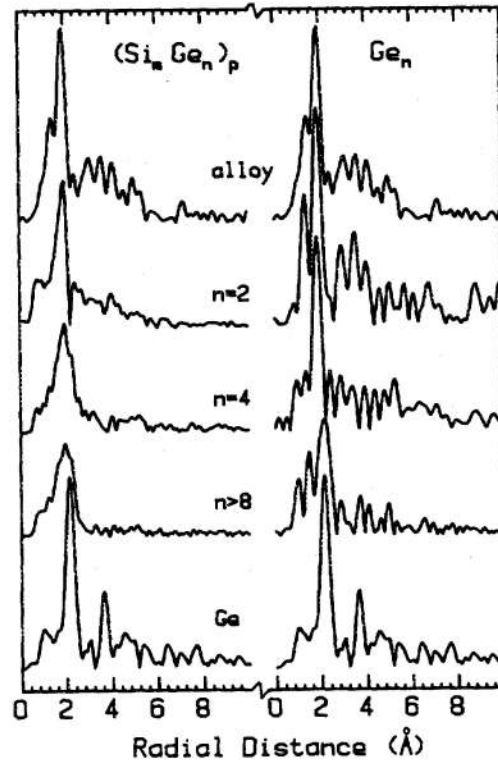
shell signal from Ge–Si bonds (at the interfaces) still produces visible effects on $\chi(k)$ and the FT. The $n=12$ single epilayer is rather Ge-like, although the more poorly defined signal above 3 Å (Fig. 3) indicates there is interdiffusion at the somewhat higher growth temperature used to prepare this sample.

The thinner layers, both ALS and single epilayer, show considerably stronger Si first shell signal, both in terms of intensity at 4 Å^{-1} and a broadening of the main radial distribution peak to lower R. While some Si first shell signal is expected in all cases, the amount is much larger than can be accounted by the proportional contribution of the Ge/Si interface layer. The excess Si contribution provides a measure of the intermixing and thus the growth quality. The extent of intermixing appears to be dependent on the growth temperature as well as on the layer thickness. Thus the $n=4$ and particularly the $n=2$ ALS, which were grown at higher temperatures than the $n=8$ ALS, have k- and R-space EXAFS signals which are progressively more similar to that of the 14 at. % Ge–Si alloy, in which almost all nearest neighbors to the Ge atoms are Si. The qualitative conclusion that there is intermixing in the $n=2$ ALS is consistent with the Raman results.[2,5] Our quantitative estimate of the amount of intermixing is presented in Sec. III C.
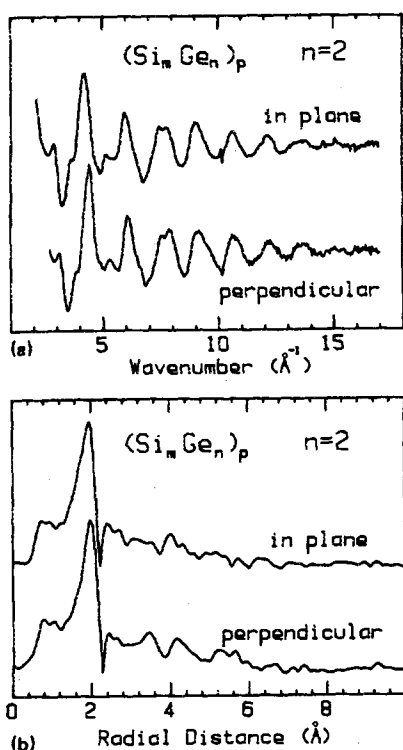
Fig. 4. (a) Ge K-edge EXAFS data for parallel and perpendicular polarization of the n = 2 (Si₆Ge₂)₄₈ multilayer ALS sample. (b) Magnitudes of the Fourier transforms of (a).

The Ge K-edge EXAFS of the $n = 4$ and $n = 2$ single layers show very strong Si first shell signal.[6] Again, a higher-than-optimum growth temperature was employed, leading to intermixing. It is noteworthy that the EY-EXAFS technique is able to provide good quality data even for two monolayers of Ge buried 500 Å inside single crystal Si.

B. Polarization dependence

Figure 4 compares spectra of the $n = 2$ ALS recorded with the sample oriented with the E vector perpendicular and parallel to the growth direction. While small differences can be seen, particularly between 2.5 and 4 Å in the FT, overall there is remarkably little polarization dependence. The polarization dependence of the other samples was even smaller. Naively one might expect the parallel polarization to have stronger contributions from Ge–Ge signal. However, the high symmetry of the diamond lattice is such that most interatomic vectors will have similar projections parallel and perpendicular to the growth direction. The sample rotation about the surface normal, which is employed to eliminate diffraction artifacts, further increases the symmetry and reduces polarization dependence. Thus for a perfect lattice there would be no polarization dependence in the first shell signal (independent of n, the layer thickness). Of course a strained Ge layer has a tetragonal distortion which should lead to a weak polarization dependence in the first

shell signal. Relative to bulk Ge the tetragonal distortion involves a contraction of the in-plane distance by 0.06 Å and an expansion of the distance along the growth direction of 0.05 Å in a fully commensurate epitaxy. A careful measurement of the first-shell polarization dependence should be able to identify whether a particular Ge epilayer is strained or relaxed.

The second (and higher) shells should exhibit a much stronger polarization dependence. One third of the atoms in the second neighbor shell are coplanar with the absorbing Ge atom. The EXAFS signal from backscattering by these in-plane atoms will contribute fully to the parallel polarization spectrum but would be extinguished in the perpendicular polarization spectrum. Since these are Ge atoms (for a perfect epitaxial layer without intermixing), there should be a considerable increase in the Ge component of the second shell signal in the parallel relative to the perpendicular orientation.

C. Preliminary quantitative analysis for the n=2 ALS

In favorable cases one can quantify the difference in two closely spaced radial distance components by analyzing the beat frequency arising from their interference.[13,14] However, the Ge–Si and Ge–Ge distances differ by less than 0.1 Å in these samples, giving rise to beating with periods longer than the range of available data. This beating does cause the abrupt drop in the first shell radial distance peak at 2.2 Å observed in the FTs of the thinner samples (Fig. 3). In order to obtain quantitative structural parameters for the Ge–Si and Ge–Ge components of the first shell signal for the $n = 2$ ALS, curve fitting has been carried out on the results from both polarizations. A symmetric Hanning filter between 0.8 and 2.8 Å was used to isolate the first shell signal. The fitting derives (N, σ, R, E_0) parameters for each of the assumed single (i.e., average) Ge–Si and Ge–Ge first shell components by optimizing the match between the Fourier filtered data and that calculated using the EXAFS expression, the derived parameters and model Ge–Si and Ge–Ge amplitude and phase functions.

The phase and amplitude functions used to simulate the Ge–Ge component were obtained from the first shell signal of pure Ge. The corresponding quantities for the Ge–Si component were taken from a spherical wave calculation[12] in which a Ge–Si distance of 2.34 Å, and 0.03 Å Debye–Waller factor was used. As always in EXAFS analysis, curve fitting must contend with strong correlations between the (N, σ) and (R, E_0) pairs of parameters for each component. In order to control this and optimize the physical validity of the results, the two polarization spectra have been analyzed simultaneously and certain of the parameters have been constrained to be identical for the two curves.

Table I presents the interatomic distances, coordination numbers and Debye–Waller factors for the Ge–Si and Ge–Ge contributions to the Fourier filtered first shell signal of the Ge K-edge spectrum of the $n = 2$ ALS for both polarizations. These results give a direct measure of both the relaxation and the degree of intermixing at the interface. The derived Ge–Si bond length [2.36(1) Å is very close to that of pure Si (2.35 Å)] while the (average) Ge–Ge bond length is

TABLE I. Structural parameters derived from curve-fit analysis of the Ge K-edge EXAFS of the $n = 2$ (Si$_6$Ge$_2$)$_{48}$ atomic layer superlattice recorded in parallel and perpendicular polarization.

Parameter	Parallel		Perpendicular	
	Ge–Si	Ge–Ge	Ge–Si	Ge–Ge
R (Å)	2.36(1)	2.43(2)	(2.36)	(2.43)[a]
N	2.84	1.16	2.76	1.24
σ (Å)	0.034	(0.034)	(0.034)	(0.034)

[a] Figures in brackets have been constrained to be identical to corresponding parameters listed earlier in the table in order to reduce the flexibility of the fit. The fourth parameter (E_0, the origin of the k scale) was allowed to vary freely for each of the four components of the overall fit. Reasonable values were found. Thus the total number of optimized parameters was reduced to 11 from the normal value of 16.

shorter than in pure Ge, consistent with that expected for a tetragonally distorted, strained Ge$_2$ epitaxial bilayer. With regard to the coordination numbers, the fit predicts a ratio of the Si:Ge first neighbors that is larger than 2. Since the expected ratio for a perfect interface is 1, the degree of intermixing predicted by the deviation is 25% i.e., one quarter of the atoms in the nominal Ge side of the interface are in fact Si and vice versa. This is in semiquantitative agreement with the estimate of $\approx 7.5\%$ provided by the Raman analysis.[2,5]

IV. CONCLUSIONS

Ge K-edge EXAFS spectroscopy has been shown to be a useful tool for characterizing the quality of MBE-grown Si-Ge superlattice structures. The extraction of accurate bond length and coordination numbers is complicated by the strong overlap in the EXAFS first-shell signal of backscattering from both the Si and Ge neighbors and by the presence of a number of different Ge environments in each sample. However progress is being made toward a quantitative analysis which promises to provide useful information on the quality of specific growths and on the structure of the ideal Si/Ge interface for various thicknesses of an embedded Ge layer.

[1] Spectroscopy of Semiconductor Microstructure, edited by G. Fasol, A. Fasolino, and P. Lugli (Plenum, New York, 1989).

[2] M. W. C. Dharma-wardana, G. C. Aers, D. J. Lockwood, and J-M. Baribeau, Phys. Rev. B 41, 5319 (1990).

[3] P. A. Lee, P. H. Citrin, P. Eisenberger, and B. M. Kincaid, Rev. Mod. Phys. 53, 769 (1981).

[4] X-ray Absorption: Principles, Techniques and Applications of EXAFS and XANES, edited by D. Konigsberger and R. Prins (Academic, New York, 1988).

[5] J-M. Baribeau, D. J. Lockwood, M. W. C. Dharma-wardana, N. L. Rowell, and J. P. McCaffrey, Thin Solid Films 183, 17 (1989).

[6] J-M. Baribeau, D. J. Lockwood, T. E. Jackman, P. Aebi, T. Tyliszczak, and A. P. Hitchcock, Can. J. Phys. (in press 1991).

[7] D. J. Lockwood and J-M. Baribeau (unpublished data).

[8] T. Tyliszczak and A. P. Hitchcock, Physica B 158, 335 (1989).

[9] A. Erbil, G. S. Cargill III, R. Frahm, and R. F. Boehme, Phys. Rev. B 37, 2450 (1988); W. T. Elam, J. P. Kikland, R. A. Neiser, and P. D. Wolf, ibid. 38, 2 (1988).

[10] T. Tyliszczak, A. P. Hitchcock, and T. E. Jackman, J. Vac. Sci. Techol. A 8, 2020 (1990).

[11] A. G. McKale, B. W. Veal, A. P. Paulikas, S. K. Chan, and G. S. Knapp, J. Am. Chem. Soc. 110, 3763 (1988).

[12] J. MustredeLeon, Y. Jacoby, E. A. Stern, and J. J. Rehr, Phys. Rev. B 42, 10843 (1990).

[13] G. Martens, P. Rabe, N. Schwentner, and A. Werner, Phys. Rev. Lett. 39, 1411 (1977).

[14] T. Sasaki, T. Onda, R. Ito, and N. Ogasawara, Jpn. J. Appl. Phys. 25, 640 (1986).